https://doi.org/10.46813/2026-164-160

UDC 624.012.35

OPTIMISATION OF THE BINDER IN THE "Na_2O-Al_2O_3-$nSiO_2$-mH_2O" SYSTEM AS A MATRIX FOR THE CONDITIONING OF LIQUID RADIOACTIVE WASTE

Sergii Guzii

State Institution "The Institute of Environmental Geochemistry of NAS of Ukraine", Kyiv, Ukraine

Email: sguziy2@gmail.com

This paper presents the results of optimizing the composition of an aluminosilicate binder based on the main structure-forming oxides SiO_2/Al_2O_3 and H_2O/Al_2O_3, with the aim of obtaining an effective matrix for the conditioning of liquid radioactive waste. It is shown that during heat treatment of the samples at temperatures of 60 and 120 °C, followed by curing under normal conditions for 7 and 28 days, the binders under consideration exhibit average densities ranging from 1.58 to 1.83 g/cm³ and compressive strengths ranging from 25 to 36 MPa, which is 5.6–8 times higher than the criterion value (Rcm > 4.5 MPa). The optimal compositions of aluminosilicate binders lie within a region bounded along the *X1* axis by a SiO_2/Al_2O_3 ratio of 7.5 to 8 mol, along the *X2* axis by an H_2O/Al_2O_3 ratio of 15 to 15.5 mol, and along the *X3* axis by a ground slag content ranging from 5 to 6 per cent. The aluminosilicate binders from the specified region belong to the mordenite type $Na_2O{\cdot}Al_2O_3{\cdot}(7.5–8)SiO_2{\cdot}(15–15.5)H_2O$ and will be used for the conditioning of boron-containing liquid radioactive waste.

INTRODUCTION

Ukraine has a powerful nuclear industry, which includes all components of the nuclear fuel cycle (NFC): from uranium mining, primary enrichment at mining and enrichment plants, to nuclear energy production at 15 NPP units, an underdeveloped processing system and a low-efficiency radioactive waste disposal system. Every year, up to tens of millions of tons of Class 1 hazardous waste are generated at NPPs; only one NPP generates about 28 t of various types of radioactive waste, of which about 20 t are spent nuclear fuel (SNF). Today, there are already problems with the storage of SNF (cubic residue of about 9,000 thousand m^3, molten salt of about 3,000 thousand t) and long-term radioactive waste (up to 80 thousand m^3). The issue of their safe conditioning and safe disposal arises. This problematic situation they be solved by expanding the use of alkaline binders as matrix systems, which will help prevent radiation threats, especially those currently emerging from the aggressor country – Russia.

Therefore, the issue of developing effective methods for handling radioactive waste (RW) is relevant, namely the introduction of effective binder systems into conditioning technologies. Conditioning of evaporated residues from reactor coolers with alkaline aluminosilicate (geocement) matrices is primarily aimed at creating compounds with stable characteristics (strength, frost resistance, radiation resistance, low porosity and leaching rate, etc.) during long periods of their storage and disposal due to chemical binding of uranium fission products, which will contribute to effective strategies for the disposal of radioactive waste.

LITERARY REVIEW AND PROBLEM STATEMENT

It should we noted that the main ideas for identifying the binding properties of alkaline elements were formulated in the late 1950s by the Ukrainian scientist V.D. Glukhovsky [1]. He discovered that alkaline activation of burnt clay rocks contributes to the formation of new formations in the hardening products, which are direct analogues of natural zeolites and feldspathoids. Such materials were called soil silicates (alkaline hydroaluminosilicates), and in modern interpretation – geocements. After 20 years, J. Davydovich somewhat expanded the idea of V.D. Glukhovsky [2, 3] in the direction of creating binders obtained by dissolving metakaolin in an alkaline medium [4–6]. He introduced the term "geopolymers", the same as geocements.

The basis for obtaining such binders is the formation of artificial zeolite-like minerals through the dissolution of powdered mineral substances rich in amorphous silica and alumina in an alkaline medium, and the polycondensation of the dissolution products into three-dimensional aluminosilicate structures. When using highly reactive metakaolin, a complete transition of amorphous silica and alumina into new formations occurs with the formation of an artificial material of monomineral composition.

Currently, more than 85 public and private research institutes worldwide are engaged in the study of geocements (geopolymers). Significant research into their development has been carried out by Ukrainian scientists: A. Baranovsky, G. Voznyuk, V. Gonchar, M. Mokhort, G. Popel and others; and by foreign researchers: T. Kriven (USA), F. Giacobello & F. Pankotti (Italy), M. Kumar (UK), P. Sturm (Netherlands), V.F.F. Barbosa (Brazil), L. Theodon (France), I. Lodeiro & A. Fernández-Jiménez (Spain), E. Vance (Australia) and others.

Research into and development of geocement (geopolymer) compositions they being conducted along the same lines as for slag-alkali binders – studies of the influence of composition [7, 8]. The fineness of grinding and the particle size distribution of the raw materials, and the curing conditions [9]. The type and content of the activator and other factors affecting the composition [10]. The influence of the composition of new formations on the properties of the binder [11]. The search for new types of raw materials [12]. The search for ways to reduce the alkali content, the improvement of technical and

operational properties through the introduction of chemical and mineral additives [13], fibres of various types and dispersibility [14, 15]; the use of various activation methods [16–20].

A conceptual model of the geocement polycondensation process they shown in Fig. 1.

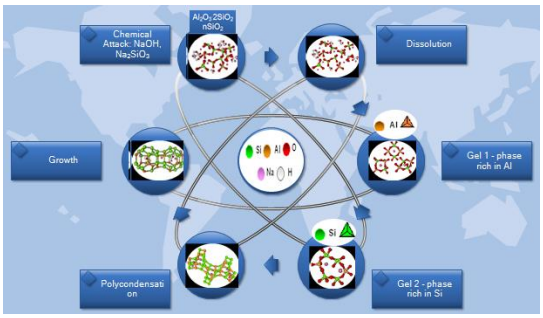


Fig. 1. Conceptual design of polycondensation process

In Figs. 2, 3, illustrate the polycondensation reactions of hydrolysed aluminate and silicate particles and the formation of a 3D geocement matrix, followed by the dissolution and hydrolysis of the aluminosilicate precursor [21].

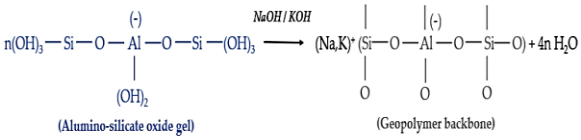


Fig. 2. Polycondensation of hydrolyzed aluminate and silicate species and formation of 3D geocement network

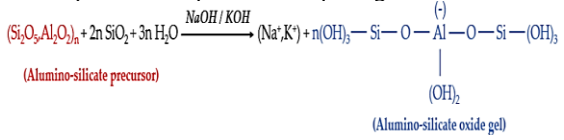


Fig. 3. Dissolution and hydrolysis reaction of the alumino-silicate precursor

More detailed information on the polycondensation processes in geocements involving the formation of zeolite-like phases such as hydronepheline $Na_2O{\cdot}Al_2O_3{\cdot}2SiO_2{\cdot}2H_2O$, natrolite $Na_2O{\cdot}Al_2O_3{\cdot}3SiO_2{\cdot}2H_2O$, analcime $Na_2O{\cdot}Al_2O_3{\cdot}4SiO_2{\cdot}2H_2O$, an artificial helandite $Na_2O{\cdot}Al_2O_3{\cdot}6SiO_2{\cdot}15H_2O$ and mordenite $Na_2O{\cdot}Al_2O_3{\cdot}8SiO_2{\cdot}15H_2O$ is presented in the works [22–26].

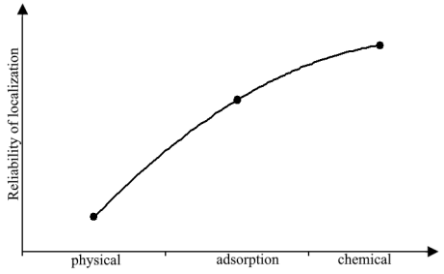


Fig. 4. The reliability of radionuclide retention depending on the nature of their interaction with cement minerals

The presence of the above-mentioned phases in geocements will facilitate the chemical binding of radionuclide ions into water-insoluble compounds (Fig. 4), which will be located in 3D unsaturated voids and held in place by electrostatic forces (Fig. 5).

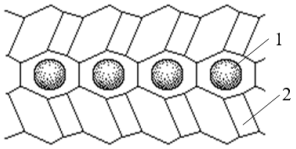


Fig. 5. Radioactive elements 'encapsulated' in the synthetic zeolite matrix of geocements: 1 – radionuclides; 2 – matrix

In geocement technology, the balance of key molar ratios determines the polycondensation of the aluminosilicate network, the formation of the gel phase, and durability [13]. The SiO_2/Al_2O_3 ratio is critical for tuning the structural and chemical properties of geocements. Adjusting this ratio using specially selected mixtures of precursors and additional silica additives significantly alters the kinetics of dissolution, hardening and strength development. A higher silica content promotes the formation of dense Si-O-Al and Si-O-Si bonds, improving compressive strength and microstructural integrity, particularly under gamma irradiation [27], by accelerating the formation of mordenite-type zeolite.

According to [27], a SiO_2/Al_2O_3 ratio in the range of 3.4–3.8 increases viscosity, improves mouldability and enhances long-term mechanical stability. Tightly cross-linked aluminosilicate networks with a higher silica content improve thermal stability, chemical resistance and resistance to freezing and thawing. Other molar ratios also play a significant role in the geopolycondensation process [27]:

- Na_2O/SiO_2 and Na_2O/Al_2O_3 are critical for regulating the alkaline environment and the dissolution of precursors, ensuring stable polycondensation;
- H_2O/Na_2O governs the kinetics of dissolution and gel formation, directly influencing workability and final strength;
- SiO_2/Na_2O regulates network connectivity and mechanical stability, with higher ratios promoting microstructural homogeneity and reducing pore connectivity.

According to [28], at a SiO_2/Al_2O_3 ratio of 2, sodalite, faujasite and EMT zeolite may appear in the reaction products of geocement. The results of MAS NMR spectroscopy of ^{29}Si and ^{27}Al indicate predominantly Si(4Al) and Al(4Si) sites, which is consistent with the presence of zeolite A, hydrosodalite, sodalite and N-A-S-H gel compared to a low SiO_2/Al_2O_3 ratio.

The study [29] examined aluminosilicate compositions with SiO_2/Al_2O_3 ratios ranging from 0.5 to 300, which were prepared from mixtures of dehydroxylated kaolinite with γ-Al_2O_3 or fine Aerosil SiO_2, at constant Na_2O/SiO_2 and H_2O/SiO_2 ratios. All compositions set at room temperature, but those with a high alumina content had low strength and did not exhibit the typical XRD and NMR characteristics of geocements. Unlike compositions with SiO_2/Al_2O_3 ratios ranging from 2 to 300. Which exhibited typical XRD patterns of an amorphous geopolymer and NMR spectra of ^{27}Al, ^{29}Si, and ^{23}Na. Samples with increasing SiO_2 content ($SiO_2/Al_2O_3 > 24$) exhibited increasingly elastic behaviour, deforming rather than fracturing brittle, and upon heating to 100…250 °C, their hydration water was

released in the form of bubbles, forming stable foamed materials at approximately 300 °C.

Using an experimental modelling tool based on the CCD method to determine the optimal influence of the components of the geocement mixture (the content of silicate SiO_2 and alumina Al_2O_3) on the strength properties of the composite, the researchers [30] established an optimal silica-to-alumina ratio of 3.7.

In a study of the behaviour of geocements as their compressive strength [31] varied as a function of curing temperature at 20 and 80 °C. As well as the molar ratios SiO_2/Al_2O_3 = 2.64–4.04 and Na_2O/Al_2O_3 = 0.62–1.54, the optimal ratios for geocement hardening at 20 °C were determined as SiO_2/Al_2O_3 = 2.96 and Na_2O/Al_2O_3 = 0.62, reaching 85 MPa after 28 days. Curing at 80 °C had a positive effect on strength development only during the first 3 days. X-ray diffraction of the geocement formulations revealed the formation of amorphous hydroaluminosilicates. The microstructure of the artificial stone consisted of unreacted quartz, metakaolinite particles and unreacted silica gel within a hydroaluminosilicate matrix. The paper [32] examines the benefits of using geocements for the immobilisation of low- and intermediate-level radioactive waste. It highlights the advantages of rapid setting, the formation of radiolytic hydrogen, fire resistance, and behaviour during freeze-thaw cycles.

Romanian researchers [33] found in their work that geocement, obtained by reacting an aluminosilicate precursor (BFS + volcanic tuff) with an alkaline activator (NaOH and Na_2SiO_3), at a SiO_2/Al_2O_3 ratio of 3.67…4.76, provides compressive strength ranging from 19.3 to 34.97 MPa.

There is evidence regarding the use of geocement, activated with NaOH and Na_2SO_3, for the immobilisation of spent ion-exchange resins and fly ash [34]. Gamma-spectrometric analysis revealed the presence of ^{40}K, ^{226}Ra and ^{232}Th in fly ash, whilst in spent ion-exchange resins, ^{134}Cs, ^{137}Cs, ^{152}Eu, ^{54}Mn, ^{58}Co, ^{60}Co, and ^{65}Zn. The incorporation of up to 10% of these wastes into the geocement matrix contributes to the production of samples with a strength of up to 6.1 MPa.

In [35], it they noted that geocement exposed to gamma radiation during setting retained satisfactory compressive strength, demonstrating high radiation resistance. This indicates that it is a promising binder for the immobilisation of waste containing Cs and Sr.

In [36, 37], it was noted that geocement of a mordenite composition and composite cement are promising binders for the conditioning of boron-containing evaporated radioactive waste.

Analysis of the information provided has shown that the most common SiO_2/Al_2O_3 ratio for producing geocements in the conditioning of evaporated liquid radioactive waste is 2–4. Geocements with a higher silica content ($SiO_2/Al_2O_3 > 10$) are technologically unsuitable for such purposes.

The aim of this study they therefore to optimise the composition of geocement in the "Na_2O-Al_2O_3-nSiO_2-mH_2O" system, intended for the conditioning of liquid radioactive waste (LRW) at a SiO_2/Al_2O_3 ratio of 4–8 and an H_2O/Al_2O_3 ratio of 15–20 at various curing and setting temperatures.

MATERIALS AND METHODS

The object of the study was alkaline composite cements of type V [38]. Alkaline aluminosilicate binders (synonym – geocements) were obtained by sol-gel synthesis technology [39–41] using the following raw materials: metakaolin (Mk), microsilica (M), liquid glass (Ms=2.6, ρ=1.36 g/cm^3) and NaOH. Adjustment of the compositions of aluminosilicate binders for the main structure-forming oxides $nSiO_2/Al_2O_3$=4–8 and mH_2O/Al_2O_3=15–20 was carried out in accordance with the recommendations [23, 25]. Ground granulated blast furnace slag (BFS) of the Mariupol Ilyich Metallurgical Plant we used as a hardener. The chemical composition of the main components of the binders we given in Table 1.

Table 1

Chemical composition of raw materials

Oxide content, %	Mk	M	BFS
SiO_2	53.42	96.0	38.28
Al_2O_3	43.8	0.47	6.52
Fe_2O_3	0.75	0.4	0.36
CaO	0.52	1.7	45.46
MgO	–	0.1	5.02
MnO	–	–	0.42
K_2O	0.75	0.2	0.45
Na_2O	0.25	0,2	0.42
Others	–	0.93	1.37
LDC	1.2	–	–

Aluminosilicate gels we obtained by dispersing solid phases in a dispersion medium with a cavitation mixer for 3 min. To determine the physical and mechanical properties, the gels of the studied compositions were poured into 3x3x3 cm molds and heat-treated at 60 and 120 °C for 4 h. Additionally, taking into account the characteristics of the conditioning of the LRW, the samples after heat treatment at 60 °C we placed in a desiccator and kept for 7 and 28 days. Optimization of the binder compositions was carried out using a three-factor simplex central planning of experiments in the mathematical environment STATISTICA 12 with the implementation of a special cubic model that takes into account the nonlinearity of the influence of factors on the properties of the initial parameters.

The coefficients of variation and the matrix for experimental design we given in Tables 2 and 3, and the implementation of the experiment this given in Tables 4 and 5.

Table 2

Variation intervals and values of variable factors

Factors, type	Natu-ral	Coded	Levels of variation		Variation interval
			0	1	
SiO_2/Al_2O_3	mole	*X1*	4	8	4
H_2O/Al_2O_3	mole	*X2*	15	20	5
BFS	%	*X3*	5	12	7

Table 3

Experiment planning matrix

Plan points	Matrix plan in codes			Full size matrix plan		
	X1	*X2*	*X3*	SiO_2/Al_2O_3	H_2O/Al_2O_3	BFS
1	0.00	1.00	0.00	4	20	5
2	0.33	0.33	0.33	5.3	16.7	7.3
3	1.00	0.00	0.00	8	15	5
4	0.50	0.50	0.00	6	17,5	5
5	0.00	0.00	1.00	4	15	12
6	0.50	0.00	0.50	6	15	8.5
7	0.00	0.00	0.50	4	17,5	8.5

Table 4

Correspondence of coded values to natural values

Coded	Natural		
	SiO_2/Al_2O_3 (*X1*)	H_2O/Al_2O_3 (*X2*)	BFS (*X3*)
0	4	15	5
0.25	5	16.25	6.75
0.5	6	17.5	8.5
0.75	7	18.75	10.25
1.0	8	20	12

Table 5

Physical and mechanical characteristics of samples of artificial stone on geocement-based

Plan points	ρ, g/cm³, after heat treatment and hardening of samples under normal conditions				R_{cm}, MPa, after heat treatment and hardening of samples under normal conditions			
	60 °C	120 °C	after 60 °C		60 °C	120 °C	after 60 °C	
			7 day	28 day			7 day	28 day
1	1.5	1.17	1.56	1.58	5.79	8.17	3.76	12.22
2	1.63	1.52	1.77	1.81	8.93	8.64	9.64	11.11
3	1.81	1.61	1.82	1.85	25.37	28.69	17.07	36.67
4	1.74	1.67	1.78	1.80	8.24	10.29	9.33	13.89
5	1.71	1.31	1.68	1.70	12.58	9.62	9.48	15.56
6	1.86	1.43	1.73	1.75	23.01	19.93	23.30	14.44
7	1.64	1.28	1.65	1.69	10.13	11.20	7.80	15.56

The physical and mechanical properties of samples from aluminosilicate binders were determined according to the current regulatory and technical documents of Ukraine [42].

RESULTS AND DISCUSSION

Because of mathematical processing of the results of experimental data (see Table 4), regression equations (1–8) we obtained, which reflect the influence of the studied factors on the change in the physical and mechanical properties of geocement samples:

$$\rho^{60}=1.81X1+1.5X2+1.71X3+0.34X1X2+0.4X1X3+0.14X2X3-3.81X1X2X3; \quad (1)$$

$$\rho^{60}{}_7=1.82X1+1.56X2+1.68X3+0.36X1X2-0.08X1X3+0.12X2X3+1.05X1X2X3; \quad (2)$$

$$\rho^{60}{}_{28}=1.85X1+1.58X2+1.7X3+0.34X1X2-0.1X1X3+0.2X2X3+1.38X1X2X3; \quad (3)$$

$$\rho^{120}=1.61X1+1.17X2+1.31X3+1.12X1X2-0.12X1X3+0.16X2X3+0.75X1X2X3; \quad (4)$$

$$R_{cm}{}^{60}=25.4X1+5.8X2+12.6X3-29.4X1X2+16.1X1X3+3.8X2X3-124.2X1X2X3; \quad (5)$$

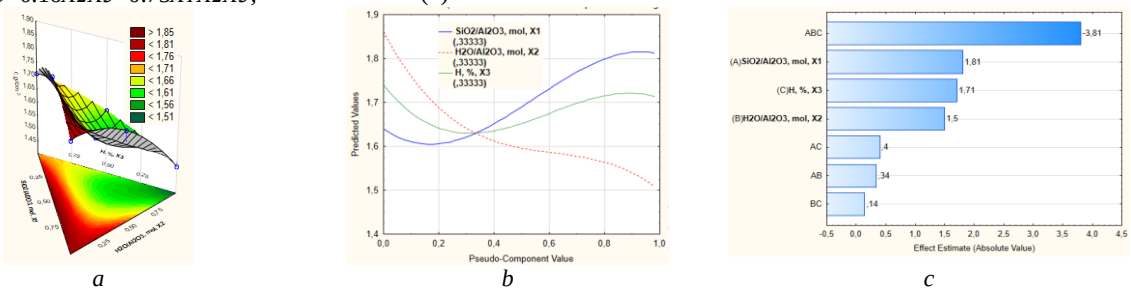
$$R_{cm}{}^{60}{}_7=17.1X1+3.8X2+9.5X3-4.3X1X2+40.1X1X3+4.7X2X3-133.9X1X2X3; \quad (6)$$

$$R_{cm}{}^{60}{}_{28}=36.67X1+12.22X2+15.56X3-42.22X1X2-46.7X1X3+6.68X2X3-33.36X1X2X3; \quad (7)$$

$$R_{cm}{}^{120}=28.7X1+8.2X2+9.6X3-32.6X1X2+3.1X1X3+9.2X2X3-124.3X1X2X3. \quad (8)$$

The response surfaces are shown in Figs. 6–13.

Analysis of equation (1) shows that the variation factors are significant, the most significant influence on the change in the density values of the samples is exerted by factors *X1* and *X3* (Fig. 6,b). Moreover, due to the joint action of these factors, 80% of the effect is achieved (Fig. 6,c); the action of factor *X2* and the products of the factors provide up to 20% of the effect. At a processing temperature of 60 °C.

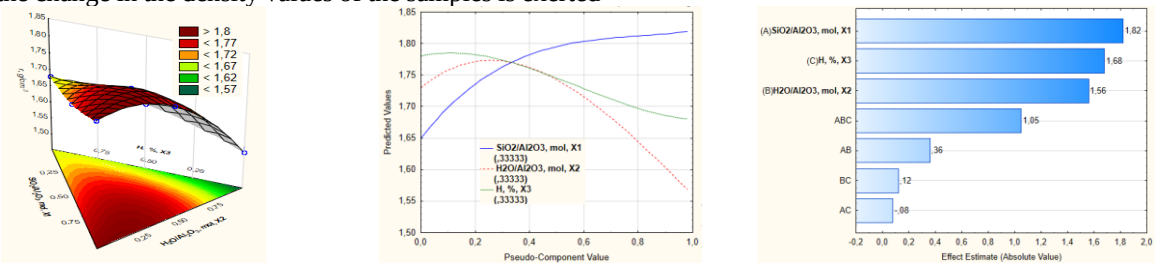


a *b* *c*

Fig. 6. Influence of variation factors on changes in density, g/cm³, of geocement samples after hardening at T=60℃: a – volumetric diagram; b – expected reactions; c – Pareto chart of effects

The isolines of maximum density values from 1.76 to 1.85 g/cm^3 (Fig. 6,a) are located in the left part of the ternary space with a simultaneous increase in the SiO_2/Al_2O_3 ratio from 4 to 8 mol (factor *X1*), the amount of slag from 5 to 12% (factor *X2*) and a decrease in the H_2O/Al_2O_3 ratio from 17.5 to 15 mol (factor *X3*).

Analysis of equation (2) shows that the variation factors are significant, the most significant influence on the change in the density values of the samples is exerted by the factors *X1*, *X3*, and *X2* (Fig. 7,b). Moreover, due to the joint action of these factors, 80% of the effect is achieved (Fig. 7,c); the joint action of the products of the factors provides up to 20% of the effect. After heat treatment at 60 °C and holding the samples for 7 days under normal conditions, it leads to a slight decrease in the density values from 1.73 to 1.82 g/cm^3 (Fig. 7,a) due to the renewal of hydrate formation in alkali aluminosilicates

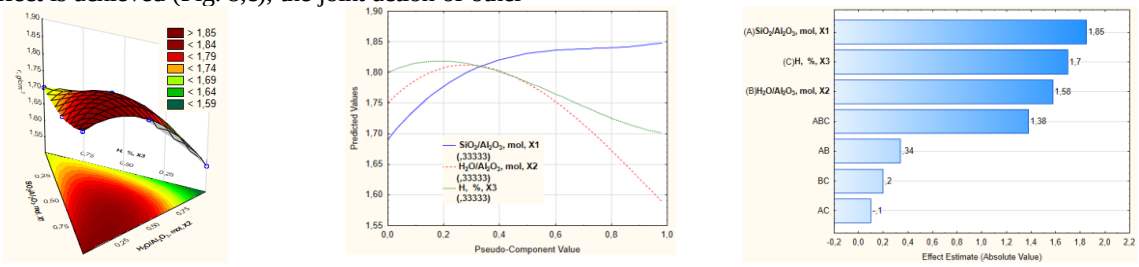


a *b* *c*

Fig. 7. Influence of variation factors on changes in density, g/cm^3, of geocement samples after hardening at T=60°C and aging for 7 days under normal conditions: a – volumetric diagram; b – expected reactions; c – Pareto chart of effects

The contours of maximum density values are located to the left of the central region of the ternary space with a simultaneous increase in the SiO_2/Al_2O_3 ratio from 5.5 to 8 mol (factor *X1*), H_2O/Al_2O_3 from 15 to 18 mol (factor *X2*) and the amount of slag from 5 to 9% (factor *X3*).

Analysis of equation (3) shows that the variation factors are significant, the most significant influence on the change in the density values of the samples is exerted by the factors *X1*, *X3*, and *X2* and the product of the factors *X1X2X3* (Fig. 8,b). Moreover, due to the joint action of these factors, 80% of the effect is achieved (Fig. 8,c); the joint action of other products of the factors provides up to 20% of the effect. After heat treatment at 60 °C and aging of the samples for 28 days under normal conditions, the density values from 1.79 to 1.85 g/cm^3 (Fig. 8,a) remain unchanged, which indicates the completion of hydrate formation in alkali aluminosilicates. The contours of maximum density values are located to the left of the central region of the ternary space with a simultaneous increase in the SiO_2/Al_2O_3 ratio from 5.2 to 8 mol (factor *X1*), H_2O/Al_2O_3 from 15 to 18 mol (factor *X2*) and the amount of slag from 5 to 9% (factor *X3*).



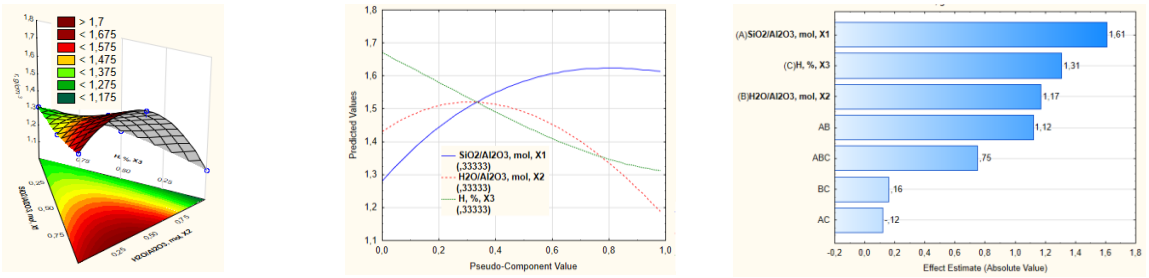
a *b* *c*

Fig. 8. Influence of variation factors on changes in density, g/cm^3, of geocement samples after hardening at T=60 °C and aging for 28 days under normal conditions: a – volumetric diagram; b – expected reactions; c – Pareto chart of effects

Analysis of equation (4) shows that the variation factors are significant, the most significant influence on the change in the density values of the samples is exerted by the factors *X1*, *X3*, and *X2* and the product of the factors *X1X2* (Fig. 9,b). Moreover, due to the joint action of these factors, 80% of the effect is achieved (Fig. 9,c); the joint action of other products of the factors provides up to 20% of the effect. After heat treatment at 120 °C, the density values are in the range from 1.58 to 1.7 g/cm^3 (Fig. 9,a), their decrease is associated with the processes of removal of physically bound water and partially hydrated water from zeolite-like new formation and low-basic calcium hydrosilicates.

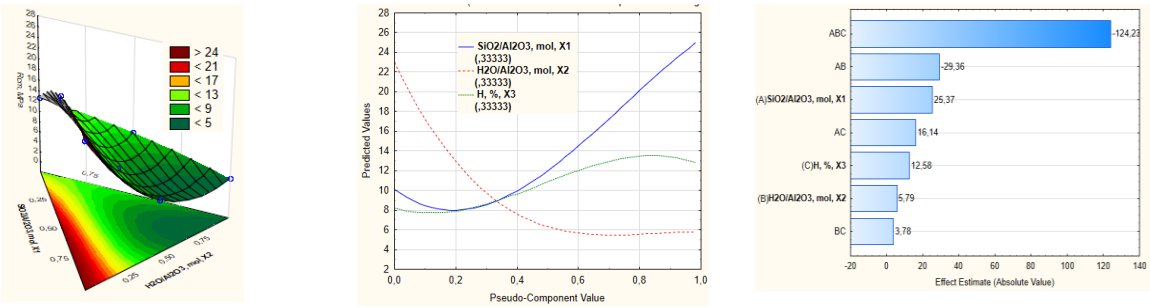
The contours of maximum density values are located to the left of the central region of the ternary space with a simultaneous increase in the SiO_2/Al_2O_3 ratio from 6.5 to 8 mol (factor *X1*), H_2O/Al_2O_3 from 15 to 17.5 mol (factor *X2*) and the amount of slag from 5 to 8% (factor *X3*).

Analysis of equation (5) shows that the variation factors are significant, the most significant influence on the change in the strength values of the samples is exerted by the factors *X1*, *X3*, and the product of the factors *X1X3* (Fig. 10,b). Moreover, due to the joint action of these factors, 80% of the effect is achieved (Fig. 10,c); the joint action of the factors *X2* and other products of the factors provide up to 20% of the effect. After heat treatment at 60 °C, the strength values are in the range from 21 to 25 MPa (Fig. 10,a). The isolines of the maximum strength values occupy a rather narrow strip, which takes place on the left side of the ternary space with a simultaneous increase in the SiO_2/Al_2O_3 ratio from 5 to 8 mol (factor *X1*), the amount of slag from 5 to 10% (factor *X3*) and a decrease in the H_2O/Al_2O_3 ratio from 16 to 15 mol (factor *X2*).



a *b* *c*

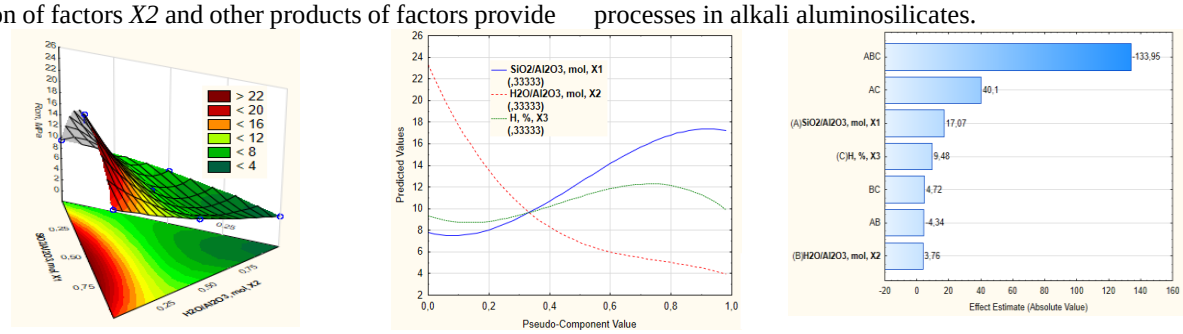
Fig. 9. Influence of variation factors on changes in density, g/cm^3, of geocement samples after hardening at T=120 °C: a – volumetric diagram; b – expected reactions; c – Pareto chart of effects



a *b* *c*

Fig. 10. Influence of variation factors on compressive strength, MPa, of geocement samples after hardening at T=60°C: a – volume diagram; b – expected reactions; c – Pareto chart of effects

Analysis of equation (6) shows that the variation factors are significant, the most significant influence on the change in the strength values of the samples is exerted by the product of factors *X1X3*, factors *X1*, and *X3* (Fig. 11,b). Moreover, due to the joint action of these factors, 80% of the effect is achieved (Fig. 11,c); the joint action of factors *X2* and other products of factors provide up to 20% of the effect. After heat treatment of the samples at 60 °C and their hardening for 7 days under normal conditions, the strength values are in the range from 20 to 22 MPa (Fig. 11,a), which is somewhat less than in the previous case. The decrease in strength is associated with the resumption of hydrate formation processes in alkali aluminosilicates.



a *b* *c*

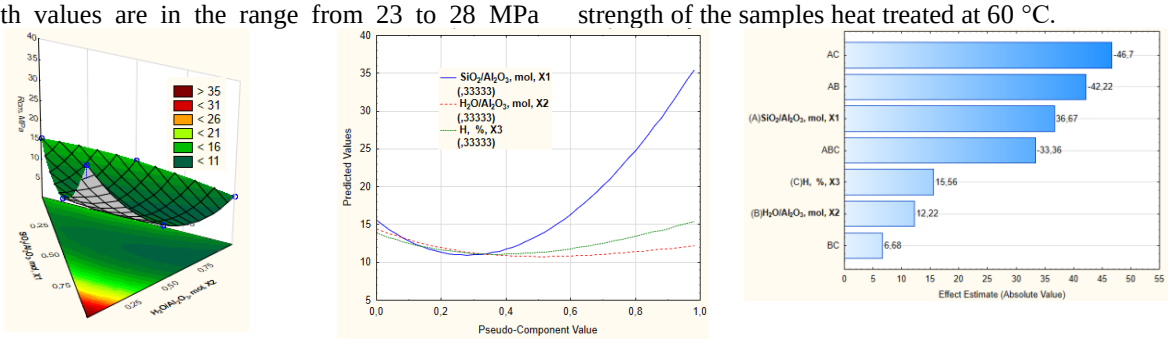
Fig. 11. Influence of variation factors on compressive strength, MPa, of geocement samples after hardening at T=60 °C and aging for 7 days under normal conditions: a – volumetric diagram; b – expected reactions; c – Pareto chart of effects

The isolines of maximum strength values occupy a rather narrow strip, which occupies a place on the left edge of the ternary space with a simultaneous increase in the SiO_2/Al_2O_3 ratio from 4.5 to 8 mol (factor *X1*), the amount of slag from 5 to 11% (factor *X3*) and a decrease in the H_2O/Al_2O_3 ratio from 16 to 15 mol (factor *X2*).

Analysis of equation (7) shows that the variation factors are significant, the most significant influence on the change in strength values is exerted by factor *X1* (Fig. 12,b), due to the action of which 80% of the effect is achieved (Fig. 12,c); the combined action of factors *X2*, *X3*, and other products of factors provide up to 20% of the effect. After heat treatment of samples at 60 °C and their hardening for 28 days under normal conditions, the strength values are in the range from 31 to 36 MPa (Fig. 12,a), which is significantly higher compared to the previous hardening period. The increase in strength is associated with the crystallization of zeolite-like neoplasms and mixed sodium-calcium aluminosilicate phases in the alkaline matrix. The isolines of maximum strength values are located in the left corner of the ternary space, the area of which is limited by the ratios of SiO_2/Al_2O_3 from 7.5 to 8 mol (factor *X1*), H_2O/Al_2O_3 from 15 to 15.75 mol (factor *X2*) and the amount of slag from 5 to 6.5% (factor *X3*).

Analysis of equation (8) shows that the variation factors are significant, the most significant influence on the change in strength values is exerted by the factor *X1*, *X3*, and the product of the factors *X2X3* (Fig. 13,b), due to the action of which 80% of the effect is achieved (Fig. 13,c); the combined action of the factors *X2* and other products of the factors provide up to 20% of the

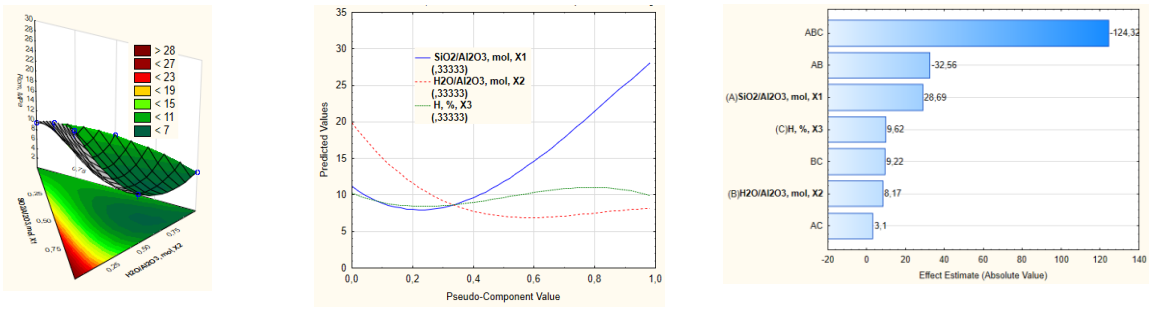
effect. After heat treatment of the samples at 120 °C, the strength values are in the range from 23 to 28 MPa (Fig. 13,a), which is significantly higher compared to the strength of the samples heat treated at 60 °C.



a *b* *c*

Fig. 12. Influence of variation factors on compressive strength, MPa, of geocement samples after hardening at T=60 °C and aging for 28 days under normal conditions: a – volumetric diagram; b – expected reactions; c – Pareto chart of effects

The increase in strength is associated with the formation of zeolite-like crystalline phases. The isolines of maximum strength values are located in the left corner of the ternary space, the area of which is limited by the ratios of SiO_2/Al_2O_3 from 6 to 8 mol (factor *X1*), H_2O/Al_2O_3 from 15 to 15.75 mol (factor *X2*) and the amount of slag from 5 to 7% (factor *X3*).



a *b* *c*

Fig. 13. Influence of variation factors on compressive strength, MPa, of geocement samples after hardening at T= 120 °C: a – volumetric diagram; b – expected reactions; c – Pareto chart of effects

The area of existence of aluminosilicate binder compositions that meets the requirements of the initial criteria we determined by the method of superimposing the response surfaces of flat diagrams (Fig. 14).

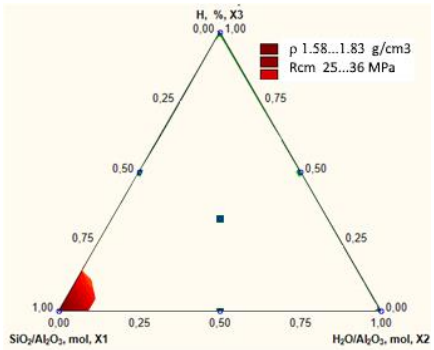


Fig. 14. Combined diagram of the influence of variation factors and processing temperatures on the change in the physical and mechanical properties of aluminosilicate binders

This area is limited on the *X1* axis by the SiO_2/Al_2O_3 ratio from 7.5 to 8 mol, on the *X2* axis by the H_2O/Al_2O_3 ratio from 15 to 15.5 mol and on the *X3* axis by the amount of ground slag from 5 to 6% aluminosilicate binders. Regardless of the processing temperatures, we characterized by a density from 1.58 to 1.83 g/cm^3 and a compressive strength from 25 to 36 MPa. Aluminosilicate binders from the specified region of composition existence belong to the mordenite type with the structural formula $Na_2O{\cdot}Al_2O_3{\cdot}(7.5–8)SiO_2{\cdot}(15–15.5)H_2O$ [9, 36] and will be used in the conditioning of boron-containing LRW [43–45].

CONCLUSIONS

Because of the work, the composition of the aluminosilicate binder we optimized according to the main structure-forming oxides and the region of existence of the compositions was determined, which corresponds to the established initial criteria. It is shown that during the heat treatment of samples at temperatures of 50 and 120 °C, and their hardening under normal conditions for 7 and 28 days, the obtained binder compositions are characterized by average density values from 1.58 to 1.83 g/cm^3 and compressive strength from 25 to 36 MPa. The optimal compositions of aluminosilicate binders are located in the region limited along the *X1* axis by the SiO_2/Al_2O_3 ratio from 7.5 to 8 mol, along the *X2* axis by the H_2O/Al_2O_3 ratio from 15 to 15.5 mol, and along the *X3* axis by the amount of ground slag from 5 to 6%. Aluminosilicate binders from the specified area belong to the mordenite type with the structural formula $Na_2O{\cdot}Al_2O_3{\cdot}(7.5–8)SiO_2{\cdot}(15–15.5)H_2O$ and will be used for conditioning boron-containing LRW.

FUNDING

The work we carried out within the framework of the state topic of NASU No. III-01-2021-2025 “Improvement of scientific principles of conditioning of liquid radioactive waste of Ukrainian NPPs to ensure long-term safety of disposal” and the Horizon-Europe project No 101166718 EURAD-2.

REFERENCES

1. V.D. Glukhovsky. *Soil silicates.* Kyiv: ”Budivelnik”, 1959, 120 p.

2. V.D. Glukhovsky. *Alkaline and alkaline-earth hydraulic binders and concretes*. Kyiv: “Vyshcha shkola”, 1979, 232 p.

3. P. Duxson, G.C. Lukey, J.S.J. Van Deventer. Physical evolution of Na-geopolymer derived from metakaolin up to 1000 // *Journal of Materials Science*. 2007, v. 42(9), p. 3044-3054.

4. J. Davidovits and M. Davidovics. Geopolymer: Ultra-High Temperature Tooling Material for the Manufacture of Advanced Composites, SAMPE Symposium // *Society for the Advancement of Material and Process Engineering*. Covina, California, USA, 1991, v. 36, 2, p. 1939-1949.

5. J. Davidovits. Proc. 2nd Intern. Conf. “Geopolymere '99”, St. Quentin, 1999.

6. J. Davidovits. *Geopolymer chemistry and applications.* Geopolymer Institute, 2008, 592 p.

7. E. Phillip, T.F. Choo, N.W.A. Khairuddin, R.O. Abdel Rahman. On the Sustainable Utilization of Geopolymers for Safe Management of Radioactive Waste: A Review // *Sustainability.* 2023, v. 15, p. 1117.

8. S. Guzii, T. Kurska, V. Andronov, M. Adamenko. Influence of Basic Oxides Ratio Li_2O/Al_2O_3, SiO_2/Al_2O_3 and H_2O/Al_2O_3 on Physical, Rheological and Colloidal-Chemical Properties of Lithium Containing Alumosilicate Suspensions in the System xLi_2O-Al_2O_3-$nSiO_2$-mH_2O // *Materials Science Forum*. 2021, v. 1038, p. 193-202.

9. H. Baykara, M.H. Cornejo, R. Murillo, et al. Preparation, characterization and reaction kinetics of green cement: Ecuadorian natural mordenite-based geopolymers // *Mater Struct*. 2017, v. 50, p. 188.

10. L. Bodnarova, S. Guzii, R. Hela, et al. Nanostructured alkaline aluminosilicate binder by carbonate mineral addition // *SSP*. 2018, v. 276, p. 192-197.

11. I. Perná, M. Nováková, D. Rimnácová, et al. The Synthesis and Characterization of Geopolymers Using Metakaolin and Mirror Glass Waste // *Appl. Sci.* 2026, v. 16, p. 667.

12. Hala A. Hossein, A.A. El-Kheshen, M.F. Zawrah. Influence of silica-fume’s addition technique and curing conditions on microstructure, physical and mechanical properties of geopolymer // *Scientific Reports*. 2025, v. 15:38486 1.

13. S.G.K. Mohan Kumar, J.M. Kinuthia, J. Oti, B.O. Adeleke. Geopolymer Chemistry and Composition: A Comprehensive Review of Synthesis, Reaction Mechanisms, and Material Properties-Oriented with Sustainable Construction // *Materials*. 2025, v. 18, p. 3823.

14. G. Tamošaitis, D. Vaiˇciukynienė, A. Kantautas, et al. Lightweight, Heat-Insulating, Alkali-Activated Slag Composites with Carbon-Based Biochar Additive and Filler // *Materials*. 2026, v. 19, p. 277.

15. P. Kryvenko, Y. Tsapko, S. Guzii, A. Kravchenko. Determination of the effect of fillers on the intumescent ability of the organic-inorganic coatings of building constructions // *Eastern-European Journal of Enterprise Technologies*. 2016, N 5(10-83), p. 26-31.

16. P. Krivenko, S. Guziy, J. Abdullah Al Musa. The influence of cavitation treatment on amorphization of kaolinite in the dispersion of the “Kaolin – Na_2O $nSiO_2$ mH_2O–NaOH–H_2O” composition // *RILEM Bookseries*. 2015, v. 10, p. 387-393.

17. P. Krivenko, S. Guzii, R. Hela. The influence of cavitation treatment on nano structuring of alkali aluminosilicate binder for intumescent coatings // *Materials Science Forum.* 2017, v. 908, p. 63-70.

18. I. Nazarenko, S. Guzii, V. Martyntsev. Intensification of hydrodynamic cavitation processes for obtaining astringents when preparing concrete mixture // *MOTROL. Commission of Motorization and Energetics in Agriculture*. 2017, v. 19, N 3, p. 89-93.

19. V. Martyntsev, S. Guzii, I. Nazarenko, V. Glyva, O. Guzii. Investigation of rheo-mechanical properties of cement suspensions activated in a hydrodynamic cavitator // *J. Technology audit and production reserves*. 2017, N 6/3(38), p. 18-25.

20. S. Guzii, P. Krivenko. The effect of hydrodynamic cavitation on performance of the alkaline aluminosilicate coatings for metal structures // *J. Materials Science: Advanced Composite Materials.* 2018, v. 2, N 2, p. 1-7.

21. M. Sambucci, A. Sibai, M. Valente. Recent Advances in Geopolymer Technology. A Potential Eco-Friendly Solution in the Construction Materials Industry: A Review // *J. Compos. Sci.* 2021, v. 5, p. 109.

22. C. Villa, E.T. Pecina, R. Torres, L. Gómez. Geopolymer synthesis using alkaline activation of natural zeolite // *Construction and Building Materials*. 2010, v. 24(11), p. 2084-2090.

23. D.W. Breck. *Zeolite Molecular Sieves: Structure. Chemistry and Use.* New York: “John Wiley & Sons”, 1974.

24. S.-M. Alexa-Stratulat, I. Olteanu, A.-M. Toma, et al. The Use of Natural Zeolites in Cement-Based Construction Materials – A State of the Art Review // *Coatings.* 2024, v. 14, p. 18.

25. R.M. Barrer. *Hydrotermal Chemistry of Zeolites*. Academic Press, London, 1982.

26. N. Ulloa, M. Jiménez, B. Serrano, C. Serrano. Natural zeolite-based geopolymers as alternative building Materials // *Revista Ingeniería de Construcción RIC*. 2022, v. 37, N 1, p. 5-13.

27. X. Chen, M. Qiu, S. Li, et al. Gamma-Ray Irradiation to Accelerate Crystallization of Mesoporous Zeolites // *Angewandte Chemie*. 2020, v. 59, N 28, p. 11325-11329.

28. P. Sturm, S. Greiser, G.J.G. Gluth, et al. Degree of reaction and phase content of silica-based one-part geopolymers investigated using chemical and NMR

spectroscopic methods // *J. Mater. Sci.* 2015, v. 50, p. 6768-6778.

29. R.A. Fletcher, K.J.D. MacKenzie, C.L. Nicholson, S. Shimada. The composition range of aluminosilicate geopolymers // *Journal of the European Ceramic Society.* 2005, v. 25, N 9, p. 1471-1477.

30. I. Bello, M.J. Kaura, O.S. Abejide, J. Ochepo, A. Bello. Models and Optimization Process of Acid Effects on the Silica and Alumina Contents of Geopolymer Concrete // *Proceedings of the 4th South American International Industrial Engineering and Operations Management Conference*. Lima, Peru, May 9-11, 2023.

31. O. Burciaga-Diaz, J.I. Escalante-Garcia, A. Gorokhovsky. Geopolymers based on a coarse low-purity kaolin mineral: Mechanical strength as a function of the chemical composition and temperature // *Cement and Concrete Composites*. 2012, v. 34, N 1, p. 18-24.

32. E.R. Vance, D.S. Perera. *Development of geopolymers for nuclear waste immobilization* / Editor(s): Michael I. Ojovan, In Woodhead Publishing Series in Energy / Handbook of Advanced Radioactive Waste Conditioning Technologies. Woodhead Publishing, 2011, p. 207-229.

33. C.M. Manolescu, C. Bucur, I. Florea, S. Lălîu. Geopolymer-based matrices for conditioning radioactive waste // *Journal of Nuclear Research and Development.* 2023, v. 26, p. 24-28.

34. N.W.A. Khairudin, M.S. Yasir, A. Ab Majid, et al. Immobilization of spent ion exchange resin from puspati triga reactor using fly ash-based geopolymer // *Malaysian Journal of Analytical Sciences.* 2015, v. 19, N 3, p. 472-480.

35. R. Lo Frano, S.A. Cancemi, E. Stefanelli, V. Dolin. Durability Assessment of Alkali-Activated Geopolymers Matrices for Organic Liquid Waste Immobilization // *Materials*. 2025, v. 18, p. 3181.

36. S.G. Guzii. Peculiarities of conditioning of evaporated boron-containing radioactive waste with aluminosilicate matrices // *Collection of scientific papers of the 18th International Scientific and Practical Conference "Academic and University Science: Results and Prospects"*, December 9-12, Poltava: Poltava Polytechnic Institute, 2025, p. 238-240.

37. A. Rozko, Y. Fedorenko, and S. Guzii. Conditioning of boron-containing LRW with composite binders // *Academic Journal Industrial Machine Building Civil Engineering*. 2025, N 1(64), p. 130-135.

38. DSTU B V.2.7-181:2009 *Building materials. Alkaline cements. Technical conditions.* Kyiv: "Ministry of Regional Development of Ukraine", 2009.

39. A. Khaleque, Md.M. Alam, M. Hoque, et al. Zeolite synthesis from low-cost materials and environmental applications: A review // *Environmental Advances.* 2020, v. 2, p. 100019.

40. A.K. Dikshit, K. Chugh, S.K. Chaturvedi, B.N. Mohapatra. Synthesis of mesoporous phase materials via Sol-gel process using Indian cementitious raw material // *Materials Today: Proceedings*. 2022, v. 62, N 2, p. 1132-1138.

41. A. Chakraborty, M. Kanti Naskar. Sol-gel synthesis of alumina gel@zeolite X nanocomposites for high performance water defluoridation: batch and column adsorption study // *Mater. Adv.* 2022, v. 3, p. 8544-8556.

42. DSTU B V.2.7-214:2009 *Building materials. Concretes. Methods for determining strength using control samples.* Kyiv: "Ministry of Regional Development of Ukraine", 2010.

43. P. He, D. Jia, M. Wang, Y. Zhou. Effect of cesium substitution on the thermal evolution and ceramics formation of potassium-based geopolymer // *Ceramics International*. 2010, v. 36(8), p. 2395-2400.

44. B. Kim, J. Lee, J. Kang, W. Um. Development of geopolymer waste form for immobilization of radioactive borate waste // *J. Hazard Mater.* 2021, v. 419, p. 26402.

45. X. Niu, Y. Elakneswaran, A. Li, et al. Incorporation of boron into metakaolin-based geopolymers for radionuclide immobilisation and neutron capture potential // *Cement and Concrete Research.* 2025, v. 190, p. 107814.

Article received 29.06.2026

ОПТИМІЗАЦІЯ В'ЯЖУЧИХ РЕЧОВИН У СИСТЕМІ «Na_2O-Al_2O_3-nSiO_2-mH_2O» ЯК МАТРИЦІ ПРИ КОНДИЦІЮВАННІ РІДКИХ РАДІОАКТИВНИХ ВІДХОДІВ

Сергій Гузій

Представлено результати оптимізації складу алюмосилікатного в'яжучого по основним структуроутворюючим оксидам SiO_2/Al_2O_3 і H_2O/Al_2O_3 з метою отримання ефективної матриці при кондиціюванні рідких радіоактивних відходів. Показано, що під час теплової обробки зразків за температур 60 і 120 °С і з їх наступним твердінням за нормальних умов на протязі 7 і 28 днів розглянуті в'яжучі характеризуються середніми значеннями щільності від 1,58 до 1,83 г/см³ і міцності при стиску від 25 до 36 МПа, що в 5.6–8 разів вище за критеріальну (Rcm > 4,5 МПа). Оптимальні склади алюмосилікатних в'яжучих знаходяться в області, що обмежена вздовж осі *X1* співвідношенням SiO_2/Al_2O_3 від 7,5 до 8 моль, вздовж осі *X2* – співвідношенням H_2O/Al_2O_3 від 15 до 15,5 моль, а вздовж осі *X3* – вмістом меленого шлаку від 5 до 6%. Алюмосилікатні в'яжучі зі зазначеної області належать до морденітового типу $Na_2O{\cdot}Al_2O_3{\cdot}(7{,}5–8)SiO_2{\cdot}(15–15{,}5)H_2O$ і будуть використовуватися для кондиціонування борвмісних рідких радіоактивних відходів.